Synthesis, Characterization, Volatility, and Thermal Stability of Fluorinated Copper(II) Aminoalkoxide Complexes as Potential Vapour Deposition Precursors

Nicholas A. Hoffman[†] *and David J. H. Emslie*[†,*]

[†] Department of Chemistry and Chemical Biology, McMaster University, 1280 Main Street West, Hamilton, Ontario, L8S 4M1, Canada.

* E-mail: emslied@mcmaster.ca. Tel: 1-905-525-9140. Web: https://emsliegroup.mcmaster.ca

ABSTRACT

The sodium aminoalkoxides Na[OCR(CF_3)CH_2NMeR'] {R = H, R' = Me (**1a**); R = R' = Me (**1b**); R = CF_3, R' = Me (**1c**); R = Me, R' = Et (**1d**); R = CF_3, R' = Et (**1e**)} were synthesized by reaction of the corresponding fluorinated epoxide {$OCH_2CR(CF_3)$; R = H (**A**), Me (**B**), CF_3 (**C**)} with a secondary amine ($HNMe_2$ or HNMeEt), followed by deprotonation with sodium hydride. Compounds **1a-e** were isolated as white powders and characterized by combustion elemental analysis and NMR spectroscopy. Epoxides **A** and **C** are commercially available, while epoxide **B** was prepared by *in-situ* deprotonation and alkylation of **A**. Reactions of **1a-e** with copper(II) chloride in THF afforded [Cu{OCR(CF_3)CH_2NMeR'}$_2$] {R = H, R' = Me (**2a**); R = R' = Me (**2b**); R = CF_3, R' = Me (**2c**); R = Me, R' = Et (**2d**); R = CF_3, R' = Et (**2e**)}; compounds **2b** and **2c** have previously been reported but not structurally characterized, while **2a**, **2d**, and **2e** are new to this report. All copper(II) compounds were characterized by combustion elemental analysis and single crystal X-ray crystallography. The physical properties of **2a-e** were also evaluated using thermogravimetric analysis (TGA), melting point, and sublimation (at 5 mTorr) data, with comparison to previously reported non-fluorinated [Cu{$OCHMeCH_2NMe_2$}$_2$] (**III**; [Cu(dmap)$_2$]).

Keywords: Copper complexes, ALD precursors, Fluorinated ligands, Aminoalkoxide ligands, Thermal stability & volatility

Introduction

Copper metal, which possesses a low resistivity and high resistance to electromigration, is traditionally used as the interconnect material for integrated circuits, which includes the nano-scale wiring to transmit electrical signals between transistors.[1] However, as the physical dimensions of transistors decrease and their complexity increases, there is growing demand for techniques to deposit ultra-thin copper films with a higher degree of uniformity, conformality, and purity.[1b, 2] Atomic layer deposition (ALD) is a thin film deposition method that can be used to deposit films which are more uniform and conformal than those accessible via other methods, such as physical vapour (PVD) and chemical vapour deposition (CVD).[3] ALD relies upon self-limiting, surface-based chemical reactions between molecules, namely a precursor and a co-reactant, which are delivered to the substrate surface in the vapour phase. Notably, an ideal ALD precursor will display high thermal stability and volatility, as well as suitable reactivity towards a given co-reactant.[3,4]

A challenge in copper metal ALD[3e,5] is the agglomeration of ultra-thin copper films at deposition temperatures above 100 °C, ultimately leading to discontinuous films.[6] Copper precursors which offer increased volatility (while maintaining high reactivity and thermal stability) are therefore of particular interest, since they could enable vapour-phase delivery into the ALD reactor at lower temperature. When comparing the known compounds bis(2,4-pentanedionato)copper(II), [Cu(acac)$_2$], and bis(1,1,1,5,5,5-hexafluoro-2,4-pentanedionato)copper(II), [Cu(hfac)$_2$] (**I** and **II** in **Figure 1**), it is notable that fluorination of the ligand backbone leads to *substantially* improved volatility.[7] Accordingly, when used as a precursor for vapour deposition, [Cu(hfac)$_2$] is deliverable at a significantly lower temperature than non-fluorinated [Cu(acac)$_2$].[8] Similar ligand fluorination strategies have been employed to increase the volatility of precursor molecules throughout the periodic table,[9] and in an extension of this line of thinking, we sought to investigate the influence of fluorination on the volatility of copper(II) aminoalkoxide complexes. Throughout academic and patent literature, a benchmark compound for low-temperature vapour deposition of copper metal, especially in the context of ALD, is the copper(II) aminoalkoxide **III** (bis(dimethylamino-2-propoxy)copper(II), [Cu(dmap)$_2$]) (**Figure 1**).[10,11,12] This compound displays high

volatility and thermal stability, making it an attractive precursor for various ALD processes.[13] A range of non-fluorinated analogues have also been described in the journal or patent literature.[10, 11b, 11c, 12b] Herein, we present the synthesis and characterization of the sodium salts of a series of fluorinated aminoalkoxide ligands, and assessment of the influence of ligand substitution on the physical properties (especially volatility and melting point) of the corresponding homoleptic copper(II) complexes, $[Cu\{OCR(CF_3)CH_2NMe_2\}_2]$ {R = H, Me or CF_3) and $[Cu\{OCR(CF_3)CH_2NMeEt\}_2]$ (R = Me or CF_3). The compounds featuring one methyl and one ethyl group on the amine donor were synthesized to explore the potential for increased ligand asymmetry to improve volatility,[14] and for longer chain alkyl substituents to afford complexes with lower melting points (ethyl substituents were used in order to minimize molecular weight, in an effort to maximize volatility, and to maintain a low degree of steric hindrance at the amine donor). Two of the five tertiary amine-containing copper complexes in this work, $[Cu\{OCR(CF_3)CH_2NMe_2\}_2]$ (R = Me and CF_3),[12e] have previously been reported, and the related fluorinated derivatives $[Cu\{OC(CF_3)_2CH_2NR_2\}_2]$ (R = allyl,[12c, 12d] CH_2CH_2OMe[12b-d]) and $[Cu\{OCH(CF_3)CH_2NR_2\}_2]$ (R = ^{n}Pr, CH_2CH_2OMe)[12c, 12d] have been described in the journal or patent literature.[12]

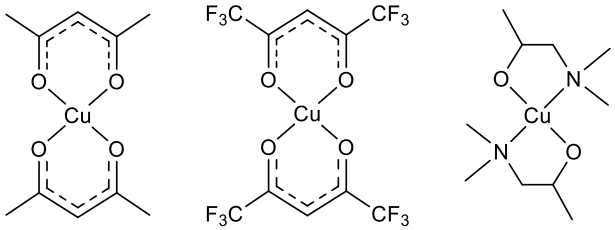

Figure 1. Select copper(II) precursors used for vapour deposition of copper metal.

Results and Discussion

The sodium aminoalkoxides, $Na[OCR(CF_3)CH_2NMeR']$ {R = H, R' = Me (**1a**); R = R' = Me (**1b**); R = CF_3, R' = Me (**1c**); R = Me, R' = Et (**1d**); R = CF_3, R' = Et (**1e**)}, were synthesized via a ring-opening

reaction of the corresponding fluorinated epoxides {$OCH_2CR(CF_3)$; R = H (**A**), Me (**B**), CF_3 (**C**)} with a secondary amine ($HNMe_2$ or HNMeEt), followed by deprotonation with sodium hydride (**Scheme 1**). Compounds **1a-e** were isolated as white powders and characterized by combustion elemental analysis and NMR spectroscopy.

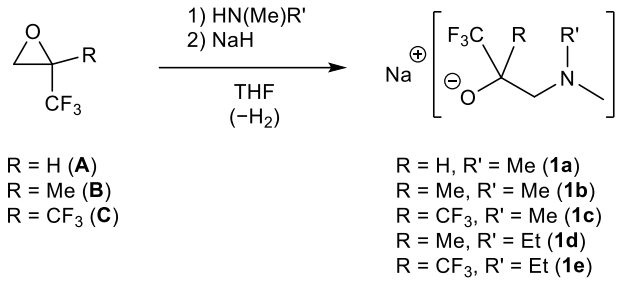

Scheme 1. Synthesis of sodium aminoalkoxide ligands **1a-e** via ring-opening of **A-C**.

The commercial availability of **A** and **C** facilitated the synthesis of **1a**, **1c** and **1e**, while epoxide **B** (required for the synthesis of **1b** and **1d**) was prepared via *in-situ* deprotonation and alkylation of **A**. This deprotonation/alkylation method[15] (**Scheme 2**) was chosen as an alternative to previous reports for the synthesis of **1b**, which utilized highly toxic and explosive diazomethane to generate **B**.[12e]

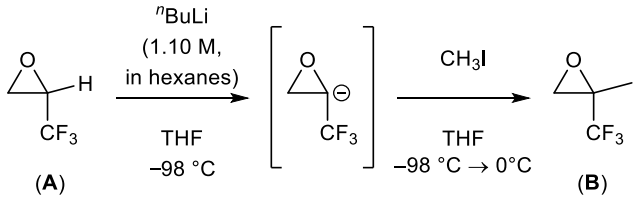

Scheme 2. *In-situ* deprotonation and alkylation of epoxide **A** to form epoxide **B**.

Reaction of sodium aminoalkoxides **1a-e** with copper(II) chloride in THF afforded the corresponding paramagnetic copper(II) complexes [$Cu\{OCR(CF_3)CH_2NMeR'\}_2$] {R = H, R' = Me (**2a**); R = R' = Me (**2b**); R = CF_3, R' = Me (**2c**); R = Me, R' = Et (**2d**); R = CF_3, R' = Et (**2e**)} in fair to good yields (**Scheme 3**). Complexes **2b** and **2c** were previously reported in the literature as potential CVD precursors,[12e] while

2a, **2d**, and **2e** are new to this report. The complexes are volatile, and can be purified by sublimation *in vacuo* (5 mTorr). All new complexes were characterized by combustion elemental analysis, melting point, and thermogravimetric analysis (*vide infra*). As **2a-e** are paramagnetic, their ^{1}H and ^{19}F NMR spectra (Figures S23 and S24) feature very broad peaks which, although they do not provide detailed structural information, can serve as a fingerprint for identification of these compounds. Compounds **2a-e** all contain tertiary alkyl amine groups, which avoids the potential for thermal decomposition involving dehydrogenation to afford an imine (which has been considered as a possible decomposition pathway for related copper(II) aminoalkoxide complexes containing secondary or primary amine groups),[12b] potentially serving to increase the thermal stability of these complexes.

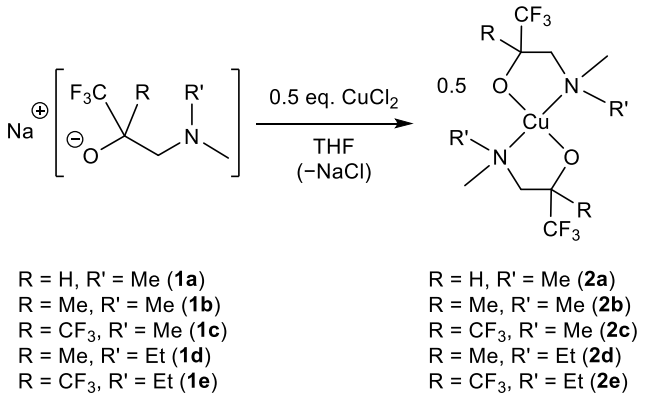

R = H, R' = Me (**1a**)
R = Me, R' = Me (**1b**)
R = CF_3, R' = Me (**1c**)
R = Me, R' = Et (**1d**)
R = CF_3, R' = Et (**1e**)

R = H, R' = Me (**2a**)
R = Me, R' = Me (**2b**)
R = CF_3, R' = Me (**2c**)
R = Me, R' = Et (**2d**)
R = CF_3, R' = Et (**2e**)

Scheme 3. Synthesis of copper(II) aminoalkoxide complexes **2a-e**.

Purple crystals of complexes **2a-e** were grown from concentrated toluene solutions and were characterized by single crystal X-ray diffraction (while **2b** and **2c** are known compounds, their crystal structures have not been previously reported). All compounds are square planar monomers, with a *trans* arrangement of the oxygen donors, and no close intermolecular contacts. In all instances except for **2d**, the copper centre is located at a special position (an inversion centre). The crystal structures of **2a-b** and **2d-e**, which contain at least one chiral centre in each ligand, exhibit some degree of disorder. However, it is notable that in both disorder components of **2a** and **2b**, the CF_3 groups are located on either side of the square plane (i.e. the molecules crystallize as *meso* (*RS*) diastereomers), and in both disorder components of **2e** the *N*-ethyl

groups are located on opposite sides of the square plane (i.e. **2e** also crystallizes as the *meso* (*RS*) diastereomer). By contrast, in both disorder components of **2d** (which has two chiral centres per ligand), (i) the CF_3 groups are located on opposite sides of the square plane and (ii) the ethyl groups are located on the same side of the square plane as each other (i.e. the alpha carbon atoms in both ligands have opposite chirality (*RS*), whereas the nitrogen atoms have the same chirality (*RR* or *SS*)); the major disorder component in the X-ray crystal structure of **2d** is shown in **Figure 2**. The Cu-O and Cu-N distances in **2a-e** (**Table 1**) range from 1.871(1)-1.887(2) Å and 2.031(1)-2.050(4) Å, respectively, which are comparable to those in other square planar copper(II) aminoalkoxide complexes (1.864(2)-1.897(2) Å and 2.017(2)-2.068(2) Å, respectively).[12e,16] The O-Cu-O and N-Cu-N bond angles in **2a-c** and **2e** are 180° due to the inversion centre at copper, whereas the square planar geometry in **2d** is slightly distorted, with O-Cu-O and N-Cu-N angles of 178.6(1)° and 178.0(1)° for the major disorder component (90%).

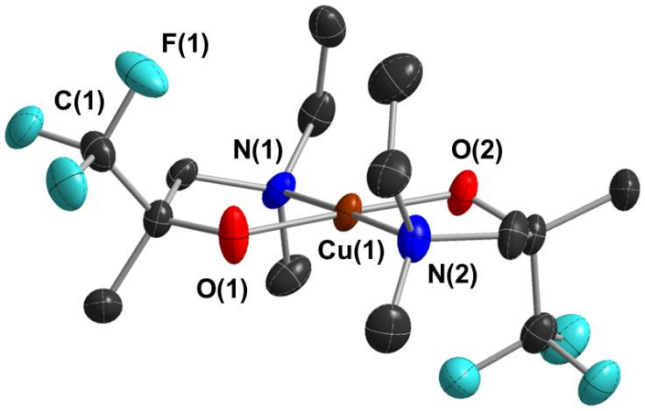

Figure 2. X-ray crystal structure of [Cu{κ^2-OCMe(CF_3)CH_2NMeEt}$_2$] (**2d**). Hydrogen atoms are omitted, and only the major disorder component (90%) is included for clarity. Thermal ellipsoids are drawn at 50% probability.

Table 1. Cu-O and Cu-N distances in the X-ray crystal structures of **2a-e**. [Disorder of the CuO_2N_2 core is observed in **2b**, **2d** and **2e**; * major disorder component (78% in **2b**; 90% in **2d**; 55% in **2e**); ** minor disorder component].

Compound	Cu-O Distance (Å)	Cu-N Distance (Å)
2a	1.871(1)	2.031(1)
2b	1.876(2)	2.049(2)* 2.050(4)**
2c	1.881(1)	2.038(1)
2d	1.875(2)-1.887(2)* 1.880(2)-1.881(2)**	2.036(2)-2.049(2)* 2.039(5)-2.041(5)**
2e	1.883(3)* 1.881(3)**	2.040(3)* 2.047(3)**

Sublimation temperatures for compounds **2a-e** are listed in **Table 2**, and provide an indication of precursor volatility, although it is important to note that these data were obtained at a pressure of 5 mTorr, which is significantly lower than that in a typical ALD experiment (commonly 0.1-1.0 Torr). To evaluate the volatility (and thermal stability) of **2a-e** in more detail, thermogravimetric analysis (TGA) of **2a-e** was conducted in an argon-filled glovebox at atmospheric pressure (**Figure 3**). The non-fluorinated copper(II) aminoalkoxide compound **III** (**Figure 1**) was also synthesized and subjected to TGA under identical experimental conditions; compound **III** has been widely employed as a highly volatile vapour deposition precursor (*vide supra*), and thus comparison of the TGA data for **2a-e** with **III** allows evaluation of the influence of ligand fluorination on precursor volatility (compound **2a** is the direct analogue of **III**, where one methyl group in **III** has been replaced by a CF_3 group).

Table 2. Summary of the thermal properties of compounds **2a-e** and **III**.

Compound	Sublimation Temperature (°C; 5 mTorr)	TGA $T_{50\%}$ (°C)	TGA Onset Temperature (°C)	TGA Residual Mass (%)	1 Torr Temperature from TGA (°C)	Melting Point (°C)
2a	50-60	178	165	0.97	125	193-195
2b	35-45	151	141	0.45	100	148-149

2c	40-50	169	156	0.23	116	184-185
2d	35-45	149	136	1.85	88	65-66
2e	40-50	161	149	0.15	103	139-140
III	35-45	151	138	1.51	97	134-135

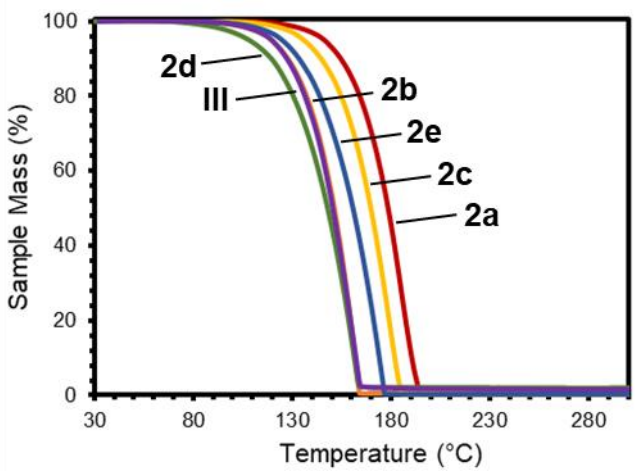

Figure 3. TGA mass loss curves for compounds **2a-e** and **III** with a heating rate of 10 °C/min at atmospheric pressure in an Ar-filled glovebox. Sample masses used: **2a** = 3.692 mg; **2b** = 3.660 mg; **2c** = 5.163 mg; **2d** = 1.925 mg; **2e** = 4.149 mg; **III** = 3.377 mg.

All six compounds (**2a-e** and **III**) display a single mass loss step in the TGA, leaving minimal residual mass, consistent with clean volatilization and thermal stability under the experimental conditions (on the short timescale of the TGA experiment). The mass loss curves of the investigated compounds are remarkably similar, with subtle differences in their volatility indicated by differing onset and 50% mass loss temperatures ($T_{50\%}$) (**Table 2**). The most asymmetric complex, **2d**, is the most volatile, while **2b** and **III** display nearly identical mass loss curves, and the direct trifluoromethyl analogue of **III**, compound **2a**, is the least volatile. The latter result is contrary to our original hypothesis that ligand fluorination would serve to improve the volatility of the corresponding copper aminoalkoxide. The temperatures at which **2a-e** and **III** would achieve a vapour pressure of 1 Torr (**Table 2**) were also calculated from the TGA data using standard methodologies (described further in the supporting information)[17] with ferrocene

as the calibrant. However, it is important to note that the calculation of a 1 Torr temperature is subject to several assumptions, and serves more as an estimate of vapour pressure that allows for comparisons to be made between similar precursors than as an absolute value.[18]

Melting points are also included in **Table 2**. When considering vapour-phase delivery, the sublimation rate of a solid precursor will be dependent on the average particle size, which will change over time.[19] In contrast, the evaporation rate of a liquid precursor should not be subject to such deviations, thereby ensuring a more consistent rate of precursor delivery. Additionally, precursors which are liquid at the delivery temperature avoid potential issues with (i) concentration of impurities at the solid surface as the precursor is consumed, hindering further volatilization,[19] (ii) the transport of fine solid particles into the reactor, and (iii) valve or delivery tube blockages caused by sublimation and deposition (the reverse process of sublimation) of a solid precursor resulting from small temperature differences within the precursor delivery vessel (anywhere between the inlet and outlet valves to/from the vessel). Thus, from a practical perspective, precursors which are liquids at the delivery temperature are highly desirable. Melting points were determined by heating a flame-sealed capillary containing **2a-e** or **III** (packed under argon) in a melting point apparatus. Comparing compound **2a** with **III** reveals that incorporation of a trifluoromethyl group on the ligand backbone serves to increase the melting point of the copper complex compared to the non-fluorinated derivative. By contrast, the melting point of **2d** (65-66 °C) is significantly lower than that of the other complexes (134-195 °C), and **2d** is also the most volatile of the species in this report, presumably due to the longer alkyl chain on nitrogen and the overall asymmetry of the ligands[14] in **2d**, rather than as a direct result of ligand trifluoromethylation.

Summary and Conclusions

A family of fluorinated copper(II) aminoalkoxide complexes, [Cu{OCR(CF_3)CH_2NMeR'}$_2$] {R = H, R' = Me (**2a**); R = R' = Me (**2b**); R = CF_3, R' = Me (**2c**); R = Me, R' = Et (**2d**); R = CF_3, R' = Et (**2e**)}, were synthesized and structurally characterized by single crystal X-ray diffraction and combustion elemental analysis. Compounds **2b** and **2c** have previously been reported, but not structurally characterized, while **2a**, **2d**, and **2e** are new to this work. The volatility, thermal stability and melting points of **2a-e** were evaluated by atmospheric pressure TGA, as well as sublimation (5 mTorr) and melting point data. For comparison, analogous measurements were also performed on the commonly employed non-fluorinated copper(II) aminoalkoxide precursor [Cu{OCHMeCH_2NMe_2}$_2$] (**III**; [Cu(dmap)$_2$]). All six compounds (**2a-e** and **III**) were found to undergo a single mass loss step in the TGA, leaving minimal residual mass, consistent with clean volatilization. Compound **2a**, which is the direct fluorinated analogue of **III** (with one CH_3 group replaced by a CF_3 group) is less volatile than **III**, with a significantly higher melting point (193-195 °C vs 134-135 °C). By contrast, **2d** is slightly more volatile than the other complexes, and has a substantially lower melting point (65-66 °C vs 134-195 °C), likely due to the longer alkyl chain on nitrogen and the overall asymmetry of the ligands, rather than as a direct result of ligand trifluoromethylation. Overall, complexes **2a-e** display sufficient volatility and thermal stability for implementation in novel vapour deposition processes, and compound **2d** offers the added benefit of a low melting point; ALD precursors which are liquid at the delivery temperature are desirable to avoid changes in the rate of precursor delivery resulting from changes in surface area, hindered volatilization due to concentration of impurities at a solid surface, transport of fine particles into the reactor, and valve or delivery tube blockages caused by sublimation and deposition (the reverse process of sublimation).

Experimental Section

General Details: An argon-filled MBraun UNIlab or Innovative Technology PureLab HE glove box equipped with a –35 °C freezer was employed for the manipulation and storage of all air-sensitive compounds, and reactions were performed on a double manifold vacuum line using standard techniques.[20]

The vacuum was measured periodically using a Kurt J. Lesker 275i convection-enhanced Pirani gauge. Residual oxygen and moisture were removed from the argon stream by passage through an Oxisorb-W scrubber from Matheson Gas Products. Centrifugation was carried out using a Benchmark Hermle Z206A centrifuge housed within a glove box.

Hexanes, toluene, diethyl ether, and tetrahydrofuran were purchased from Sigma-Aldrich, and deuterated solvents were purchased from Cambridge Isotope Laboratories. Solvents were initially dried and distilled at atmospheric pressure from sodium/benzophenone (hexanes, diethyl ether, tetrahydrofuran, C_6D_6, d_8-THF) or sodium (toluene). All solvents were stored over sodium/benzophenone and introduced to reactions or solvent storage flasks via vacuum transfer with condensation at −78 °C. Epoxides **A** and **B** were purchased from SynQuest Laboratories and distilled to solvent storage flasks via vacuum transfer with condensation at −78 °C prior to use. Complex **III** was synthesized according to literature procedures.[10a] Dimethylamine (2.0 M in THF), *N*-ethylmethylamine, methyl iodide, sodium hydride, ^{n}BuLi (1.6 M in hexanes), copper(II) chloride, and copper(II) methoxide were purchased from Sigma-Aldrich and used without further purification. 1-Dimethylamino-2-propanol was purchased from Sigma-Aldrich and dried over 4 Å molecular sieves and distilled to a solvent storage flask via vacuum transfer with condensation at −78 °C.

NMR spectroscopy was performed on a Bruker AV-600 spectrometer. All ^{1}H NMR and ^{13}C NMR spectra were referenced relative to $SiMe_4$ through the C_6D_6 or d_8-THF resonance or the protio impurity in the C_6D_6 or d_8-THF solvent: 7.16 and 3.58 ppm, respectively, for ^{1}H NMR and 128.06 and 67.21 ppm, respectively for ^{13}C NMR. ^{19}F NMR spectra were referenced by indirect referencing from a ^{1}H NMR spectrum.[21] Peak assignments in the spectra of all new diamagnetic compounds were made with the aid of DEPT-q, COSY, HSQC and HMBC experiments.

Single-crystal X-ray crystallographic analyses were performed on crystals coated in Paratone oil and mounted on either a Bruker SMART APEX II diffractometer with a 3 kW sealed tube Mo generator and APEX II CCD detector or a STOE IPDS II diffractometer with an image plate detector in the McMaster Analytical X-ray Diffraction Facility. Raw data was processed using XPREP (as part of the

APEX v2.2.0 software) and solved by an intrinsic method (SHELXT).[22] In all cases, non-hydrogen atoms were refined anisotropically. Hydrogen atoms were either located from the distance map or generated in ideal positions and then updated with each cycle of refinement, which was performed with SHELXL in OLEX2-1.5.[23,24]

Combustion elemental analyses were performed by Midwest Microlabs in Indianapolis, Indiana or at the University of Calgary using a Perkin Elmer Model 2400 series II analyzer. Thermogravimetric analysis was performed by Green Centre Canada in Kingston, Ontario using a TA Instruments Discovery TGA located within an argon-filled glove box. Melting point determinations were performed by packing the analyte into a flame-sealed pipette and sealing the open face of the pipette with Apiezon H-grease inside an argon-filled glovebox. The pipette was then removed from the glovebox and quickly flame-sealed (below the grease but sufficiently distant from the analyte) to form a sealed capillary, which was in turn used for analysis using a DigiMelt Melting Point Apparatus.

Synthetic Details:

$Na[OCH(CF_3)CH_2NMe_2]$ (1a): Under an inert atmosphere, 0.806 g (7.19 mmol) of 2-(trifluoromethyl)oxirane (**A**) was charged to a 25 mL flask containing 5 mL of THF. The flask was cooled to 0 °C and 7.91 mmol of dimethylamine (4.52 mL of a 1.75 M solution in THF) was added dropwise with stirring. The reaction was stirred for 30 minutes at 0 °C, followed by stirring at room temperature for 14 hours. The solvent and excess dimethylamine were removed at 0 °C *in vacuo* to yield 0.991 g (6.31 mmol) of a white crystalline powder. This powder was redissolved in 5 mL of THF, and the resulting solution was added dropwise to a cooled (0 °C) 50 mL flask containing 0.167 g (6.94 mmol) of sodium hydride suspended in 10 mL of THF. The reaction mixture was stirred for 4 hours at room temperature and then evaporated to dryness *in vacuo*. Excess sodium hydride was removed by centrifugation after addition of 5 mL of THF, and the resultant solution was evaporated to dryness *in vacuo* to yield 1.064 g (5.94 mmol) of **1a** as a white powder (83% yield from **A**). This product is pure by NMR spectroscopy, and was used in all subsequent reactions. However, elemental analysis was carried

out on crystals obtained by dissolving a sample of **1a** in a 3:1 mixture of hot toluene and THF, followed by cooling to −35 °C. ^{1}H NMR (d$_8$-THF, 600 MHz, 298 K): δ 4.19-4.24 (*m*, 1H, C*H*(CF$_3$)), 2.35 (*t*, 1H, $^{2}J_{H,H}/^{3}J_{H,H}$ = 10.8 Hz, C*H*$_2$), 2.23 (*s*, 6H, N(C*H*$_3$)$_2$), 2.03 (*d*, 1H, $^{2}J_{H,H}$ = 10.8 Hz, C*H*$_2$). ^{13}C{^{1}H} NMR (d$_8$-THF, 151 MHz, 298 K): δ 129.89 (*q*, $^{1}J_{C,F}$ = 287.4 Hz, *C*F$_3$), 72.40 (*q,* ^{2}J$_{C,F}$ = 25.4 Hz, *C*(CF$_3$)), 65.59 (*s*, *C*H$_2$), 45.83 (*s*, N(*C*H$_3$)$_2$). ^{19}F NMR (d$_8$-THF, 565 MHz, 298 K): δ −82.29 (*d*, $^{3}J_{F,H}$ = 4.0 Hz, C*F*$_3$). Anal. Calcd. for C$_5$H$_9$F$_3$NNaO (%): C, 33.52; H, 5.07; N 7.82. Found: C, 33.53; H, 5.04; N, 7.50.

Na[OCMe(CF$_3$)CH$_2$NMe$_2$] (1b): Under an inert atmosphere, 2.120 g (18.92 mmol) of 2-(trifluoromethyl)oxirane (**A**) was charged to a 250 mL flask containing 100 mL of THF and subsequently cooled to −98 °C. A 1.10 M solution of ^{n}BuLi in hexanes (20 mL; 22.00 mmol) was then added dropwise over the course of 15 minutes. This solution was stirred for an additional 10 minutes at −98 °C, whereupon 4.600 g (32.41 mmol) of methyl iodide was added . The reaction mixture was stirred for 1 hour at −98 °C and then for an additional hour at −78 °C, whereupon the reaction temperature was raised to 0 °C. 70 mmol of dimethylamine (40.00 mL of 1.75 M solution in THF) was then added slowly, and the reaction was stirred for 30 minutes at 0 °C, followed by stirring at room temperature for 14 hours. The reaction mixture was then quenched with 90 mL of a saturated ammonium chloride solution, the organic layer separated, and the aqueous layer extracted with 3 x 50 mL of diethyl ether. All organic layers were combined, washed with 80 mL of a brine solution, and dried with magnesium sulfate. Solvent was removed on a rotary evaporator, and the residual orange oil was distilled under vacuum to yield 3.191 g of a clear, colourless oil. This oil was then dissolved in 5 mL of dry and degassed THF and added dropwise to a 0 °C suspension of sodium hydride (0.491 g; 21.00 mmol) in 40 mL of THF. The mixture was stirred for 4 hours at room temperature, filtered, and the filtrate was evaporated to dryness *in vacuo* to yield 2.467 g (13.00 mmol) of **1b** as a white solid (68% yield from **A**). This product is pure by NMR spectroscopy, and was used in all subsequent reactions. However, elemental analysis was carried out on crystals obtained by dissolving a sample of **1b** in hot toluene, followed by cooling to −35 °C. ^{1}H NMR (d$_8$-THF, 600 MHz,

298 298 K): δ 2.43-2.46 (*m*, 1H, CH_2), 2.33 (*s*, 6H, N(CH_3)$_2$), 2.19-2.23 (*m*, 1H, CH_2), 1.16 (*s*, 3H, CH_3).
299 ^{13}C{^{1}H} NMR (d$_8$-THF, 151 MHz, 298 K): δ 131.06 (*q*, $^1J_{C,F}$ = 297.0 Hz, *C*F$_3$), 75.48 (br *s*, *C*(CF$_3$)),
300 69.15, 69.08 (2 × *m*, *C*H$_2$)†, 49.41, 49.33, 49.26 (3 × *m*, N(*C*H$_3$)$_2$)†, 26.25, 26.16, 26.09 (3 × *m*, *C*H$_3$)†. ^{19}F
301 NMR (d$_8$-THF, 565 MHz, 298 K): δ −83.85, –83.95, –84.00 (3 × *m*, C*F*$_3$)†. Anal. Calcd. for C$_6$H$_{11}$F$_3$NNaO
302 (%): C, 37.30; H, 5.75; N 7.25. Found: C, 37.76; H, 6.13; N, 7.18. † Multiple peaks are likely due to
303 diastereomers resulting from aggregation.
304
305 **Na[OC(CF$_3$)$_2$CH$_2$NMe$_2$] (1c):** Under an inert atmosphere, 1.878 g (10.43 mmol) of 2,2-
306 bis(trifluoromethyl)oxirane (**C**) was charged to a 25 mL flask containing 5 mL of THF. The flask was
307 cooled to 0 °C and 11.47 mmol of dimethylamine (6.55 mL of a 1.75 M solution in THF) was added
308 dropwise with stirring. The reaction was stirred for 30 minutes at 0 °C, followed by stirring at room
309 temperature for 14 hours. The solvent and excess dimethylamine were removed at 0 °C *in vacuo* to yield
310 1.744 g (7.74 mmol) of a clear, light yellow oil. This oil was dissolved in 5 mL of THF and added dropwise
311 to a cooled (0 °C) 50 mL flask containing 0.204 g (8.52 mmol) of sodium hydride suspended in 10 mL of
312 THF. The reaction mixture was stirred for 4 hours at room temperature and then evaporated to dryness *in*
313 *vacuo*. Excess sodium hydride was removed by centrifugation after addition of 5 mL of THF, and the
314 resultant solution was evaporated to dryness *in vacuo* to yield 1.830 g (7.40 mmol) of **1c** as a white powder
315 (71% yield from **C**). This product is pure by NMR spectroscopy, and was used in all subsequent reactions.
316 However, elemental analysis was carried out on crystals obtained by dissolving a sample of **1c** in hot
317 toluene, followed by cooling to −35 °C. ^{1}H NMR (d$_8$-THF, 600 MHz, 298 K): δ 2.52 (*s*, 2H, CH_2), 2.31
318 (*s*, 6H, N(CH_3)$_2$). ^{13}C{^{1}H} NMR (d$_8$-THF, 151 MHz, 298 K): δ 127.62 (*q*, $^1J_{C,F}$ = 294.7 Hz, *C*F$_3$), 81.63
319 (*sept*, $^2J_{C,F}$ = 23.6 Hz, *C*(CF$_3$)$_2$), 62.70 (*s*, *C*H$_2$), 48.62 (*s*, N(*C*H$_3$)$_2$). ^{19}F NMR (d$_8$-THF, 565 MHz, 298
320 K): δ −79.38 (*s*, C*F*$_3$). Anal. Calcd. for C$_6$H$_8$F$_6$NNaO (%): C, 29.16; H, 3.27; N 5.67. Found: C, 29.20;
321 H, 3.40; N, 5.63.
322

Na[OCMe(CF$_3$)CH$_2$NMeEt] (1d): Under an inert atmosphere, 0.918 g (8.20 mmol) of 2-(trifluoromethyl)oxirane (**A**) was charged to a 100 mL flask containing 40 mL of THF and subsequently cooled to −98 °C. A 1.10 M solution of ^{n}BuLi in hexanes (8.20 mL; 9.02 mmol) was then added dropwise over the course of 10 minutes. This solution was stirred for an additional 10 minutes at −98 °C, whereupon 2.287 g (16.11 mmol) of methyl iodide was added. The reaction mixture was stirred for 1 hour at −98 °C and stirred for an additional hour at −78 °C, whereupon the reaction temperature was raised to 0 °C. 32.00 mmol of *N*-ethylmethylamine (18.30 mL of a 1.75 M solution in THF) was then added slowly, and the reaction was stirred for 30 minutes at 0 °C, followed by stirring at room temperature for 14 hours. The reaction mixture was then quenched with 40 mL of a saturated ammonium chloride solution, the organic layer separated, and the aqueous layer extracted with 3 x 20 mL of diethyl ether. All organic layers were combined, washed with 40 mL of a brine solution, and dried with magnesium sulfate. Solvent was removed on a rotary evaporator, and the residual orange oil distilled under vacuum to yield 1.248 g (6.74 mmol) of a clear, colourless oil. This oil was then dissolved in 5 mL of dry and degassed THF and added dropwise to a 0 °C suspension of sodium hydride (0.178 g; 7.42mmol) in 15 mL of THF. The mixture was stirred for 4 hours at room temperature, filtered, and evaporated to dryness *in vacuo* to yield 1.166 g (5.63 mmol) of **1d** as a white solid (69% yield from **A**). This product is pure by NMR spectroscopy, and was used in all subsequent reactions. However, elemental analysis was carried out on crystals obtained by cooling a concentrated toluene solution of **1d** to −35 °C. ^{1}H NMR (d$_8$-THF, 600 MHz, 298 K): δ 2.51-2.55 (*m*, 2H, N(C*H*$_2$CH$_3$)), 2.36 (*s*, 2H, C*H*$_2$), 2.31 (*s*, 3H, N(C*H*$_3$), 1.16 (*s*, 3H, C*H*$_3$), 1.02 (*t*, 3H, $^3J_{H,H}$ = 7.1 Hz, N(CH$_2$C*H*$_3$)). ^{13}C{^{1}H} NMR (d$_8$-THF, 151 MHz, 298 K): δ 131.28 (*q*, $^1J_{C,F}$ = 293.6 Hz, *C*F$_3$), 75.44 (*q*, $^2J_{C,F}$ = 22.1 Hz, *C*(CF$_3$)), 67.59* (*C*H$_2$), 55.00 (*s*, N(*C*H$_2$CH$_3$), 44.31 (*s*, N(*C*H$_3$)), 25.99 (*s*, *C*H$_3$), 11.95 (*s*, N(CH$_2$*C*H$_3$)). ^{19}F NMR (d$_8$-THF, 565 MHz, 298 K): δ −83.18, –83.21, –83.26, –83.34, −83.47 (5 × *m*, C*F*$_3$)†. Anal. Calcd. for C$_7$H$_{13}$F$_3$NNaO (%): C, 40.57; H, 6.34; N 6.76. Found: C, 40.40; H, 6.53; N, 6.70. * Peak obscured by d^8-THF solvent signal, identified by ^{1}H-^{13}C HSQC. † Multiple peaks are likely due to diastereomers resulting from aggregation.

Na[OC(CF$_3$)$_2$CH$_2$NMeEt] (1e): Under an inert atmosphere, 0.500 g (2.78 mmol) of 2,2-bis(trifluoromethyl)oxirane (**C**) was charged to a 25 mL flask containing 5 mL of THF. The flask was cooled to 0 °C and 3.06 mmol of *N*-ethylmethylamine (1.75 mL of a 1.75 M solution in THF) was added dropwise with stirring. The reaction was stirred for 30 minutes at 0 °C, followed by stirring at room temperature for 14 hours. The solvent and excess *N*-ethylmethylamine were removed at 0 °C *in vacuo* to yield 0.622 g (2.77 mmol) of a clear, light-yellow oil. This oil was dissolved in 5 mL of THF and added dropwise to a cooled (0 °C) 50 mL flask containing 0.072 g (3.00 mmol) of sodium hydride suspended in 10 mL of THF. The reaction mixture was stirred for 4 hours at room temperature and then evaporated to dryness *in vacuo*. Excess sodium hydride was removed by centrifugation after addition of 5mL of THF, and the resultant solution was evaporated to dryness *in vacuo* to yield 0.667 g (2.55 mmol) of **1e** as a white powder (92% yield from **C**). This product is pure by NMR spectroscopy, and was used in all subsequent reactions. However, elemental analysis was carried out on crystals obtained by cooling a concentrated toluene solution of **1e** to −35 °C. ^{1}H NMR (d$_8$-THF, 600 MHz, 298 K): δ 2.57 (*s*, 2H, C*H*$_2$), 2.51 (*q*, 2H, $^3J_{H,H}$ = 7.2 Hz, N(C*H*$_2$CH$_3$)), 2.32 (*s*, 3H, N(C*H*$_3$)), 1.01 (*t*, 3H, $^3J_{H,H}$ = 7.2 Hz, N(CH$_2$C*H*$_3$)). ^{13}C{^{1}H} NMR (d$_8$-THF, 151 MHz, 298 K): δ 127.68 (*q*, $^1J_{C,F}$ = 295.3 Hz, *C*F$_3$), 81.61 (br *s*, *C*(CF$_3$)$_2$), 60.81 (*s*, *C*H$_2$), 54.49 (*s*, N(*C*H$_2$CH$_3$)), 44.35 (*s*, N(*C*H$_3$)), 12.13 (*s*, N(CH$_2$*C*H$_3$)). ^{19}F NMR (d$_8$-THF, 565 MHz, 298 K): δ −79.26 (*s*, C*F*$_3$). Anal. Calcd. for C$_7$H$_{13}$F$_3$NNaO (%): C, 32.19; H, 3.87; N 5.36. Found: C, 32.27; H, 4.07; N, 5.34.

[Cu{OCH(CF$_3$)CH$_2$NMe$_2$}$_2$] (2a): In an argon-filled glovebox, a solution containing 0.484 g (2.70 mmol) of **1a** in 5 mL of THF was added to a stirring suspension of CuCl$_2$ (0.182 g; 1.35 mmol) in 5 mL of THF. The reaction mixture was stirred for 16 hours, filtered, and evaporated to dryness *in vacuo* to yield a purple solid, which was purified by sublimation under vacuum (50-60 °C, 5 mTorr) to yield 0.262 g (0.70 mmol) of **2a** as a purple, crystalline solid (52% yield). X-ray quality crystals of **2a** were obtained

by cooling a concentrated toluene solution to −35 °C. ^{1}H NMR (C_6D_6, 600 MHz, 298 K): δ ~24 (br *s*), ~14 (br *s*). ^{19}F NMR (C_6D_6, 565 MHz, 298 K): δ ~(−58) (br *s*). Melting Point: 193-195 °C. Anal. Calcd. for $C_{10}H_{18}CuF_6O_2N_2$ (%): C, 32.09; H, 4.65; N 7.82. Found: C, 31.95; H, 4.84; N, 7.46.

[Cu{OCMe(CF$_3$)CH$_2$NMe$_2$}$_2$] (2b): In an argon-filled glovebox, a solution containing 2.135 g (11.00 mmol) of **1b** in 10 mL of THF was added to a stirring suspension of $CuCl_2$ (0.740 g; 5.50 mmol) in 10 mL of THF. The reaction mixture was stirred for 16 hours, filtered, and evaporated to dryness *in vacuo* to yield a purple solid, which was purified by sublimation under vacuum (35-45 °C, 5 mTorr) to yield 1.922 g (4.76 mmol) of **2b** as a purple crystalline solid (87% yield). X-ray quality crystals of **2b** were obtained by cooling a concentrated toluene solution to −35 °C. ^{1}H NMR (C_6D_6, 600 MHz, 298 K): δ ~15 (br *s*). ^{19}F NMR C_6D_6, 565 MHz, 298 K): δ ~(−86) (br *s*). Melting Point: 148-149 °C. Anal. Calcd. for $C_{12}H_{22}CuF_6O_2N_2$ (%): C, 35.44; H, 5.84; N 6.77. Found: C, 35.69; H, 5.49; N, 6.94.

[Cu{OC(CF$_3$)$_2$CH$_2$NMe$_2$}$_2$] (2c): In an argon-filled glovebox, a solution containing 0.727 g (2.94 mmol) of **1c** in 5 mL of THF was added to a stirring suspension of $CuCl_2$ (0.198 g; 1.47 mmol) in 5 mL of THF. The reaction mixture was stirred for 16 hours, filtered, and evaporated to dryness *in vacuo* to yield a purple solid, which was purified by sublimation under vacuum (40-50 °C, 5 mTorr) to yield 0.558 g (1.09 mmol) of **2c** as a purple crystalline solid (74% yield). X-ray quality crystals of **2c** were obtained by cooling a concentrated toluene solution to −35 °C. ^{1}H NMR (C_6D_6, 600 MHz, 298 K): No observable signals in the range of +/− 100 ppm. ^{19}F NMR (C_6D_6, 565 MHz, 298 K): δ ~(−68) (br *s*). Melting Point: 184-185 °C. Anal. Calcd. for $C_{12}H_{16}CuF_{12}O_2N_2$ (%): C, 27.99; H, 3.42; N 5.31. Found: C, 28.16; H, 3.15; N, 5.47.

[Cu{κ^2-OCMe(CF$_3$)CH$_2$NMeEt}$_2$] (2d): In an argon-filled glovebox, a solution containing 0.829 g (4.00 mmol) of **1d** in 5 mL of THF was added to a stirring suspension of $CuCl_2$ (0.269 g; 2.00 mmol) in 5 mL of THF. The reaction mixture was stirred for 16 hours, filtered, and evaporated to dryness *in vacuo* to

yield a purple solid, which was purified by sublimation under vacuum (35-45 °C, 5 mTorr) to yield 0.694 g (1.61 mmol) of **2d** as a purple crystalline solid (81% yield). X-ray quality crystals of **2d** were obtained by cooling a concentrated hexanes solution to −35 °C. ^{1}H NMR (C_6D_6, 600 MHz, 298 K): δ ~18 (br *s*), ~11 (br *s*), ~10 (br *s*), ~8 (br *s*), ~7 (br *s*), ~3 (br *s*), ~2 (br *s*). ^{19}F NMR (C_6D_6, 565 MHz, 298 K): δ ~(−70) (br *s*), ~(−87) (br *s*). Melting Point: 65-66 °C. Anal. Calcd. for $C_{14}H_{26}CuF_6O_2N_2$ (%): C, 39.06; H, 6.25; N, 6.60. Found: C, 38.92; H, 6.08; N, 6.49.

[Cu{OC(CF$_3$)$_2$CH$_2$NMeEt}$_2$] (2e): In an argon-filled glovebox, a solution containing 0.522 g (2.00 mmol) of **1e** in 5 mL of THF was added to a stirring suspension of $CuCl_2$ (0.134 g; 1.00 mmol) in 5 mL of THF. The reaction mixture was stirred for 16 hours, filtered, and evaporated to dryness *in vacuo* to yield a purple solid, which was purified by sublimation under vacuum (40-50 °C, 5 mTorr) to yield 0.419 g (0.78 mmol) of **2e** as a purple crystalline solid (78% yield). X-ray quality crystals of **2e** were obtained by cooling a concentrated toluene solution to −35 °C. ^{1}H NMR (C_6D_6, 600 MHz, 298 K): δ ~20 (br *s*), ~15 (br *s*), ~2 (br *s*). ^{19}F NMR (C_6D_6, 565 MHz, 298 K): δ ~(−59) (br *s*), ~(−65) (br *s*), ~(−70) (br *s*). Melting Point: 139-140 °C. Anal. Calcd. for $C_{14}H_{20}CuF_{12}O_2N_2$ (%): C, 31.24; H, 3.60; N, 5.17. Found: C, 31.14; H, 3.74; N, 5.19.

ASSOCIATED CONTENT

Data Availability. ^{1}H, ^{13}C{^{1}H}, ^{19}F and selected 2D NMR spectra, and general X-ray crystal structure data and refinement details are provided in the Supporting Information. CCDC 2324430-2324434 contain the supplementary crystallographic data for compounds **2a**-**2e**, respectively. These data can be obtained, free of charge, via www.ccdc.cam.ac.uk/data_request/cif (or from the Cambridge Crystallographic Data Centre, 12 Union Road, Cambridge CB2 1EZ, UK; fax: +44 1223 336033; or email: deposit@ccdc.cam.ac.uk).

COMPETING INTERESTS

There are no competing interests to declare.

ACKNOWLEDGMENT

D.J.H.E. thanks NSERC of Canada for a Discovery grant (RGPIN-2020-06794), and the Ontario government for an Ontario Research Fund Research Excellence grant (ORF-RE-09-051). We are also grateful to Dr. Robert G. Syvret and EFC Gases and Advanced Materials for their contributions to the ORF-RE grant. N.A.H. thanks NSERC of Canada for CGS-M and PGS-D scholarships, and the Ontario government for an Ontario Graduate Fellowship (OGF). We are grateful to Dr. Yurij Mozharivskyj for access to his X-ray diffractometer, and Dr. Jeffrey S. Price for assistance with X-ray crystallography.

REFERENCES

(1) (a) Li, Z.; Tian, Y.; Teng, C.; Cao, H. Recent Advances in Barrier Layer of Cu Interconnects. *Materials* **2020**, *13* (21), 5049. (b) Kim, H.-W. Recent Trends in Copper Metallization. *Electronics* **2022**, *11* (18), 2914. (c) Moon, J. H.; Jeong, E.; Kim, S.; Kim, T.; Oh, E.; Lee, K.; Han, H.; Kim, Y. K. Materials Quest for Advanced Interconnect Metallization in Integrated Circuits. *Adv. Sci.* **2023**, *10* (23), 2207321.

(2) (a) Leskelä, M.; Ritala, M. Atomic Layer Deposition Chemistry: Recent Developments and Future Challenges. *Angew. Chem. Int. Ed.* **2003**, *42* (45), 5548-5554. (b) Kim, H. The application of atomic layer deposition for metallization of 65 nm and beyond. *Surf. Coat. Technol.* **2006**, *200* (10), 3104-3111.

(3) (a) Vidjayacoumar, B.; Emslie, D. J. H.; Clendenning, S. B.; Blackwell, J. M.; Britten, J. F.; Rheingold, A. Investigation of $AlMe_3$, BEt_3, and $ZnEt_2$ as Co-Reagents for Low-Temperature Copper Metal ALD/Pulsed-CVD. *Chem. Mater.* **2010**, *22* (17), 4844-4853. (b) Knisley, T. J.; Kalutarage, L. C.; Winter, C. H. Precursors and chemistry for the atomic layer deposition of metallic first row transition metal films. *Coord. Chem. Rev.* **2013**, *257* (23), 3222-3231. (c) Miikkulainen, V.; Leskelä, M.; Ritala, M.; Puurunen, R. L. Crystallinity of inorganic films grown by atomic layer deposition: Overview and general trends. *J. Appl. Phys.* **2013**, *113* (2), 021301. (d) Hagen, D. J.; Pemble, M. E.; Karppinen, M. Atomic layer

deposition of metals: Precursors and film growth. *Appl. Phys. Rev.* **2019**, *6* (4), 041309. (e) Gordon, P. G.; Kurek, A.; Barry, S. T. Trends in Copper Precursor Development for CVD and ALD Applications. *ECS J. Solid State Sci. Technol.* **2015**, *4* (1), N3188.

(4) Devi, A. 'Old Chemistries' for new applications: Perspectives for development of precursors for MOCVD and ALD applications. *Coord. Chem. Rev.* **2013**, *257* (23), 3332-3384.

(5) Tripathi, T. S.; Wilken, M.; Hoppe, C.; de los Arcos, T.; Grundmeier, G.; Devi, A.; Karppinen, M. Atomic Layer Deposition of Copper Metal Films from $Cu(acac)_2$ and Hydroquinone Reductant. *Adv. Eng. Mater.* **2021**, *23* (10), 2100446.

(6) (a) Dai, M.; Kwon, J.; Halls, M. D.; Gordon, R. G.; Chabal, Y. J. Surface and Interface Processes during Atomic Layer Deposition of Copper on Silicon Oxide. *Langmuir* **2010**, *26* (6), 3911-3917. (b) Park, K.-M.; Kim, J.-K.; Han, B.; Lee, W.-J.; Kim, J.; Shin, H.-K. Influence of the deposition temperature on the properties of copper thin films prepared by alternating injection of $Cu(ethylketoiminate)_2$ and H_2 on a ruthenium substrate. *Microelectron. Eng.* **2012**, *89*, 27-30. (c) Hagen, D. J.; Connolly, J.; Povey, I. M.; Rushworth, S.; Pemble, M. E. Island Coalescence during Film Growth: An Underestimated Limitation of Cu ALD. *Adv. Mater. Interfaces* **2017**, *4* (18), 1700274. (d) Yao, Y.; Chen, B.; Zaera, F. On the Mechanism of the Atomic Layer Deposition of Cu Films on Silicon Oxide Surfaces: Activation Using Atomic Hydrogen and Three-Dimensional Growth. *Chem. Mater.* **2023**, *35* (5), 2155-2164.

(7) Fahlman, B. D.; Barron, A. R. Substituent effects on the volatility of metal β-diketonates. *Adv. Mater. Opt. Electron.* **2000**, *10* (3-5), 223-232.

(8) Bernal Ramos, K.; Saly, M. J.; Chabal, Y. J. Precursor design and reaction mechanisms for the atomic layer deposition of metal films. *Coord. Chem. Rev.* **2013**, *257* (23), 3271-3281.

(9) Donald, C. B.; Halina, C.; Michael, B. H.; Majid, M.; Ruowen, W. Fluorinated tertiary alkoxides of some lanthanides: tris-trifluorotertiarybutoxides of lanthanum, praseodymium and europium. *Polyhedron* **1993**, *12* (24), 2955-2960.

(10) (a) Becker, R.; Weiß, J.; Winter, M.; Merz, K.; Fischer, R. A. New heterometallic copper zinc alkoxides: synthesis, structure properties and pyrolysis to Cu/ZnO composites. *J. Organomet. Chem.*

2001, *630* (2), 253-262. (b) Baum, T. H.; Bhandari, G.; Xu, C. Chemical vapor deposition precursors for deposition of copper. US6822107B1, 2004.

(11) For literature discussing the synthesis of non-fluorinated derivatives of [Cu(dmap)$_2$] which contain a tertiary amine, see: (a) Park, J. W.; Jang, H. S.; Kim, M.; Sung, K.; Lee, S. S.; Chung, T.-M.; Koo, S.; Kim, C. G.; Kim, Y. Synthesis of Cu(II) aminoalkoxide complexes and their unusual thermolysis to Cu(0). *Inorg. Chem. Commun.* **2004**, *7* (4), 463-466. (b) Kim, Y.; Kim, C. G.; Chung, T.-M.; Lee, S. S.; An, K.-S.; Yang, T. S.; Jang, H. S. Volatile copper aminoalkoxide complex and deposition of copper thin film using same. US6982341B1, 2006. (c) Tomaharu, Y.; Masaki, E.; Atsushi, S.; Akihiro, N.; Makoto, O. Copper Compound, Starting Material for Forming Thin Film, and Method for Manufacturing Thin Film. US2017044188A1, 2017.

(12) For literature discussing the synthesis of derivatives of [Cu(dmap)$_2$] containing a primary or secondary amine, see: (a) Chang, I.-S.; Willis, C. J. Fluorinated alkoxides. Part XI. Studies on highly fluorinated amino-alcohols and their metal derivatives. *Can. J. Chem.* **1977**, *55* (13), 2465-2472. (b) Hsu, P. F.; Chi, Y.; Lin, T. W.; Liu, C. S.; Carty, A. J.; Peng, S. M. Self-Reducible Cu^{II} Source Reagents for the CVD of Copper. *Chem. Vap. Depos.* **2001**, *7* (1), 28-31. (c) Peng-Fu, H.; Lin, T.-W.; Liun, C.-S.; Carty, A. J. Self-reducible and self-decomposing copper metalorganic complexes for deposition of electric conducting copper metal films. WO2001094291A1, 2001. (d) Chi, Y.; Hsu, P.-F.; Lin, T.-W.; Liu, C.-S.; Carty, A. J. Self-reducible copper(II) source reagents for chemical vapor deposition of copper metal. US6369256B1, 2002. (e) Chi, Y.; Hsu, P.-F.; Liu, C.-S.; Ching, W.-L.; Chou, T.-Y.; Carty, A. J.; Peng, S.-M.; Lee, G.-H.; Chuang, S.-H. Fluorinated aminoalkoxide Cu^{II} complexes: new CVD precursors for deposition of copper metal. *J. Mater. Chem.* **2002**, *12* (12), 3541-3550.

(13) For literature discussing new copper ALD processes with [Cu(dmap)$_2$], see: (a) Lee, B. H.; Hwang, J. K.; Nam, J. W.; Lee, S. U.; Kim, J. T.; Koo, S.-M.; Baunemann, A.; Fischer, R. A.; Sung, M. M. Low-Temperature Atomic Layer Deposition of Copper Metal Thin Films: Self-Limiting Surface Reaction of Copper Dimethylamino-2-propoxide with Diethylzinc. *Angew. Chem. Int. Ed.* **2009**, *48* (25), 4536-4539. (b) Knisley, T. J.; Ariyasena, T. C.; Sajavaara, T.; Saly, M. J.; Winter, C. H. Low Temperature Growth

of High Purity, Low Resistivity Copper Films by Atomic Layer Deposition. *Chem. Mater.* **2011**, *23* (20), 4417-4419. (c) Kalutarage, L. C.; Clendenning, S. B.; Winter, C. H. Low-Temperature Atomic Layer Deposition of Copper Films Using Borane Dimethylamine as the Reducing Co-reagent. *Chem. Mater.* **2014**, *26* (12), 3731-3738. (d) Väyrynen, K.; Mizohata, K.; Räisänen, J.; Peeters, D.; Devi, A.; Ritala, M.; Leskelä, M. Low-Temperature Atomic Layer Deposition of Low-Resistivity Copper Thin Films Using $Cu(dmap)_2$ and Tertiary Butyl Hydrazine. *Chem. Mater.* **2017**, *29* (15), 6502-6510.

(14) For select examples of the influence of ligand asymmetry on precursor volatility and/or melting point, see: (a) Park, K.-H.; Marshall, W. J. Remarkably Volatile Copper(II) Complexes of N,N'-Unsymmetrically Substituted 1,3-Diketimines as Precursors for Cu Metal Deposition via CVD or ALD. *J. Am. Chem. Soc.* **2005**, *127* (26), 9330-9331. (b) Baunemann, A.; Lemberger, M.; Bauer, A. J.; Parala, H.; Fischer, R. A. MOCVD of TaN Using the All-Nitrogen-Coordinated Precursors $[Ta(NEtMe)_3(N\text{-}tBu)]$, $[Ta(NEtMe)(N\text{-}tBu)\{C(N\text{-}iPr)_2(NEtMe)\}_2]$, and $[Ta(NMeEt)_2(N\text{-}tBu)\{Me_2N\text{-}N(SiMe_3)\}]$. *Chem. Vap. Depos.* **2007**, *13* (2-3), 77-83. (c) Eleter, M.; Daniele, S.; Brize, V.; Dubourdieu, C.; Lachaud, C.; Blasco, N.; Pinchart, A. Remarkable Influence of molecular structure of N,N'-unsymmetrically substituted 1,3-amidinate and -guanidinate on the Volatility and the Thermal Stability of Precursors for HfO_2 Films via Liquid Injection-MOCVD. *ECS Trans.* **2009**, *25* (8), 151. (d) Chen, T.; Xu, C.; Baum, T. H.; Stauf, G. T.; Roeder, J. F.; DiPasquale, A. G.; Rheingold, A. L. New Tantalum Amido Complexes with Chelate Ligands as Metalorganic (MO) Precursors for Chemical Vapor Deposition (CVD) of Tantalum Nitride Thin Films. *Chem. Mater.* **2010**, *22* (1), 27-35. (e) Krasnopolski, M.; Hrib, C. G.; Seidel, R. W.; Winter, M.; Becker, H.-W.; Rogalla, D.; Fischer, R. A.; Edelmann, F. T.; Devi, A. Homoleptic Gadolinium Amidinates as Precursors for MOCVD of Oriented Gadolinium Nitride (GdN) Thin Films. *Inorg. Chem.* **2013**, *52* (1), 286-296. (f) Lubitz, K.; Sharma, V.; Shukla, S.; Berthel, J. H. J.; Schneider, H.; Hoßbach, C.; Radius, U. Asymmetrically Substituted Tetrahedral Cobalt NHC Complexes and Their Use as ALD as well as Low-Temperature CVD Precursors. *Organometallics* **2018**, *37* (7), 1181-1191. (g) Soussi, K.; Mishra, S.; Jeanneau, E.; Mantoux, A.; Daniele, S. Synthesis, characterization and thermal transport properties of heteroleptic N-alkyl triazenide complexes of titanium(IV) and niobium(V). *Polyhedron*

528 **2018**, *152*, 84-89. (h) Gakiya-Teruya, M.; Jiang, X.; Le, D.; Üngör, Ö.; Durrani, A. J.; Koptur-Palenchar,
529 J. J.; Jiang, J.; Jiang, T.; Meisel, M. W.; Cheng, H.-P.; et al. Asymmetric Design of Spin-Crossover
530 Complexes to Increase the Volatility for Surface Deposition. *J. Am. Chem. Soc.* **2021**, *143* (36), 14563-
531 14572. (i) Samii, R.; Buttera, S. C.; Kessler, V.; O'Brien, N. J. Synthesis, Structure and Thermal Properties
532 of Volatile Indium and Gallium Triazenides. *Eur. J. Inorg. Chem.* **2022**, *2022* (24), e202200161.
533 (15) Yamauchi, Y.; Katagiri, T.; Uneyama, K. The First Generation and Stereospecific Alkylation of α-
534 Trifluoromethyl Oxiranyl Anion. *Org. Lett.* **2002**, *4* (2), 173-176.
535 (16) Goel, S. C.; Kramer, K. S.; Chiang, M. Y.; Buhro, W. E. Preparation and x-ray crystal structures of
536 volatile copper(II) alkoxides. *Polyhedron* **1990**, *9* (4), 611-613.
537 (17) Kunte, G. V.; Shivashankar, S. A.; Umarji, A. M. Thermogravimetric evaluation of the suitability of
538 precursors for MOCVD. *Meas. Sci. Technol.* **2008**, *19* (2), 025704.
539 (18) Barry, S. T. *Chemistry of Atomic Layer Deposition*; De Gruyter, 2022.
540 (19) Koponen, S. E.; Gordon, P. G.; Barry, S. T. Principles of precursor design for vapour deposition
541 methods. *Polyhedron* **2016**, *108*, 59-66.
542 (20) Burger, B. J.; Bercaw, J. E. Vacuum Line Techniques for Handling Air-Sensitive Organometallic
543 Compounds. In *Experimental Organometallic Chemistry*, ACS Symposium Series, Vol. 357; American
544 Chemical Society, 1987; pp 79-115.
545 (21) Harris, R. K.; Becker, E. D.; Menezes, S. M. C. d.; Goodfellow, R.; Granger, P. NMR nomenclature.
546 Nuclear spin properties and conventions for chemical shifts (IUPAC Recommendations 2001). *Pure Appl.*
547 *Chem.* **2001**, *73* (11), 1795-1818.
548 (22) Sheldrick, G. SHELXT - Integrated space-group and crystal-structure determination. *Acta*
549 *Crystallographica Section A* **2015**, *71* (1), 3-8.
550 (23) Sheldrick, G. Crystal structure refinement with SHELXL. *Acta Crystallographica Section C* **2015**,
551 *71* (1), 3-8.
552 (24) Dolomanov, O. V.; Bourhis, L. J.; Gildea, R. J.; Howard, J. A. K.; Puschmann, H. OLEX2: a
553 complete structure solution, refinement and analysis program. *J. Appl. Crystallogr.* **2009**, *42* (2), 339-341.

554